Article

Drone Control in AR: An Intuitive System for Single-Handed Gesture Control, Drone Tracking, and Contextualized Camera Feed Visualization in Augmented Reality

Konstantinos Konstantoudakis [*,†], Kyriaki Christaki [*,†], Dimitrios Tsiakmakis, Dimitrios Sainidis, Georgios Albanis, Anastasios Dimou [*] and Petros Daras

Visual Computing Lab (VCL), Centre for Research and Technology-Hellas (CERTH), Information Technologies Institute (ITI), 57001 Thessaloniki, Greece; tsiakmakis@iti.gr (D.T.); dsainidis@iti.gr (D.S.); galbanis@iti.gr (G.A.); daras@iti.gr (P.D.)

* Correspondence: k.konstantoudakis@iti.gr (K.K.); kchristaki@iti.gr (K.C.); dimou@iti.gr (A.D.)

† These authors contributed equally to this work.

Abstract: Traditional drone handheld remote controllers, although well-established and widely used, are not a particularly intuitive control method. At the same time, drone pilots normally watch the drone video feed on a smartphone or another small screen attached to the remote. This forces them to constantly shift their visual focus from the drone to the screen and vice-versa. This can be an eye-and-mind-tiring and stressful experience, as the eyes constantly change focus and the mind struggles to merge two different points of view. This paper presents a solution based on Microsoft's HoloLens 2 headset that leverages augmented reality and gesture recognition to make drone piloting easier, more comfortable, and more intuitive. It describes a system for single-handed gesture control that can achieve all maneuvers possible with a traditional remote, including complex motions; a method for tracking a real drone in AR to improve flying beyond line of sight or at distances where the physical drone is hard to see; and the option to display the drone's live video feed in AR, either in first-person-view mode or in context with the environment.

Keywords: drones; augmented reality; AR; gesture recognition

check for updates

Citation: Konstantoudakis, K.; Christaki, K.; Tsiakmakis, D.; Sainidis, D.; Albanis, G.; Dimou, A.; Daras, P. Drone Control in AR: An Intuitive System for Single-Handed Gesture Control, Drone Tracking, and Contextualized Camera Feed Visualization in Augmented Reality. *Drones* **2022**, *6*, 43. https://doi.org/10.3390/drones6020043

Academic Editors: Diego González-Aguilera and Pablo Rodríguez-Gonzálvez

Received: 31 December 2021
Accepted: 1 February 2022
Published: 10 February 2022

1. Introduction

Over the past decade commercial drones, and quadcopters in particular, have become increasingly popular and affordable. In addition to their use in professional or casual photography, they have grown into a transformative force in diverse sectors, including inspection [1,2], mapping [3,4], exploration [5], human–machine interaction [6], search-and-rescue missions [7,8], and more. More recently, their combination with virtual and augmented reality (VR and AR, respectively) has yielded new experiences such as first-person-view (FPV) fights (www.dji.com/gr/dji-fpv, accessed on 20 December 2021), AR training (vrscout.com/news/dronoss-training-drone-pilots-with-ar/, accessed on 20 December 2021), and mixed reality games (www.dji.com/newsroom/news/edgybees-launches-the-first-augmented-reality-game-for-dji-drone-users, accessed on 20 December 2021).

Learning to pilot a quadcopter effectively can be a challenging task: Conventional remote controllers are largely unintuitive, as they use two joysticks to control flight, with one corresponding to horizontal motions (pitch and roll) and the other to vertical (throttle) and rotational (yaw) motions. Additional wheels and buttons control the drone's camera. While basic motions in relaxed circumstances are achievable with short training sessions, complex motions can be more difficult. Moreover, in challenging or stressful circumstances (e.g., in disaster response or under tight time constraints), the lack of intuitive controls add additional cognitive load on the pilot, affecting his/her safety and efficiency. In addition, the remote controller in itself, requiring the continuous use of both hands, can be restrictive. Although alternative remote controllers, such as the DJI motion controller, provide a less cumbersome solution, they cannot support the full range of motions executable by a traditional remote.

Another challenge stems from the difference in position and orientation between the drone and its pilot, which can make it difficult to match the drone's camera feed with the pilot's surroundings. In particular, especially when the drone is at some distance or out of direct line of sight, it can be challenging both to judge its position and orientation and have a direct understanding of where its camera is pointing at. Moreover, as the video feed is normally displayed on a screen attached to the remote, it requires users to constantly change their focus from the drone (in the air) to the screen (usually held at chest level, hence towards the ground), glancing from one to the other. This can be both tiring (mentally as well as visually) and adds to the cognitive load, as the user alternates between two different points of view. Although VR FPV mode eliminates the change of perspective, it leaves users unaware of their own surroundings, which can be prohibitive in many cases.

In this paper, we propose an AR solution that leverages gesture recognition, computer vision AI, and motion tracking techniques to provide a natural user interface for intuitive drone control and contextualized information visualization. Based on the Microsoft HoloLens 2 headset (https://www.microsoft.com/en-us/hololens/hardware, accessed on 20 December 2021), the presented system allows users to pilot a drone using single-hand gestures, improves tracking the position of the drone in an AR environment, and provides video feed visualization in either the contextualized or FPV modes. It allows for a comfortable flight, as both hands are free and can be used for other tasks when not directing the drone. AR tracking improves drone visibility in longer distances or in low light conditions. The visualization of the drone's video feed in the AR display means that users can view both the video and their surroundings without glancing towards different directions. In conjunction with tracking, a contextualized video view projects the video in the approximate location and/or direction of its contents, considering the drone's location and orientation, resulting in a mixed reality view combining the virtual video feed with the real world. The main contributions of this work are as follows:

- Gesture control for drones, supporting all drone and camera motions, including complex motions;
- Drone tracking in AR, based on cumulative Inertial Measurement Unit (IMU) readings and an initial relative pose calibration, while exploring visual-based drift correction;
- Visualization of the drone's camera feed in AR in context with the real world, considering the relative pose between drone and user, with the additional option to explore and integrate depth estimation for more accurate placement.
- A unified solution encompassing all of the above, consisting of a HoloLens 2 user interface app, an Android UAV interface app, and a Kafka message broker.

The rest of the paper is organized as follows: Section 2 discusses earlier work related to the presented solution, in particular regarding drone gesture control, drone tracking, and the visualization of information in AR; Section 3 presents the system's architecture, including hardware, software, communication, and data flow; Section 4 describes the primary technical tasks that were needed to realize the solution; Section 5 discusses the testing of the system, including subjective and objective measurements and feedback; and finally, Section 6 summarizes this work and outlines possible future developments.

2. Related Work

2.1. Gesture Control

With the ever growing accessibility of drones and the range of their potential applications, the users acting as pilots are no longer limited to highly-trained professionals. This, in turn, leads to a shift in the design of human–drone interfaces as there is a need for simplified control methods [9] that provide an easy way to control a drone without the need of extensive training. There are now several approaches that go beyond the standard remote controller with joysticks and allow the user to use inherent expression and communication means such as gesture, touch, and speech. These methods are also known as Natural User Interfaces (NUI) and have the advantage, in some application domains, to feel intuitive and require less training time and cognitive effort. Suárez Fernández et al. [10] implemented and tested a gesture drone control interface utilizing a LeapMotion sensor (https://www.ultraleap.com/product/leap-motion-controller/, accessed on 20 December 2021). At the early stages of our work, we applied a similar approach using LeapMotion, but later, we abandoned this plan for more efficient AR interfaces. Herrmann and Schmidt [11] designed and evaluated an NUI for drone piloting based on gestures and speech in AR. Their study results indicate that the use of the designed NUI is not more effective and efficient than the use of a conventional remote controller. However, the selected gesture "alphabet" may have played a crucial role on the study results. For example, their input alphabet included combinations of head and hand movement in order to perform certain navigation tasks, something that many users of the study found confusing. In our approach, although head gestures do exist, they are not combined with hand gestures, and they are only used to perform auxiliary tasks in certain navigation modes. In their survey about human–drone interactions, Tezza and Andujar [9] classify gesture interaction as an intuitive and easy to learn control interface but with the disadvantages of high latency and low precision. However, we argue that the current technologies for gesture recognition are able to overcome the aforementioned disadvantages.

2.2. Tracking

Positional or motion tracking is the ability of a device to estimate its position in relation to the environment around it or the world coordinate system. As described by Kleinschmidt et al. [12], there are two fundamental solutions for positional tracking, marker- and non-marker-based methods. Marker-based methods require the use of standard tags such as ARTags and QR codes for the coupling between an agent's camera and the tracked element. In our application both approaches are available since each one has certain pros and cons: Our current non-marker-based approach does not require the use of tags, however, it requires a two-step calibration process. Marker-based approaches are used in time-critical tasks or in hostile environments where there is no sufficient time for calibration, however, they can only be performed with drones that are already equipped with the compatible tags. Regardless of the approach used, the tracking process is prone to the accumulation of errors and latency, and is in general computationally intensive. Several methods attempt to overcome these challenges. Islam et al. [13] introduced an indoor tracking system with a rotary-laser base station and photo-diode sensors on tracking objects. The base station scans the space and detects the UAV sufficiently. The error is almost negligible as the estimation in 5 m is only 13 cm. Arreola et al. [14] proposed a position estimation method using a low-cost GPS and optical flows provided by UAV's camera. This approach is available only outdoors since the system uses GPS measurements. In a hybrid case, Tsai and Zhuang [15] adapted optical flow and ultrasonic sensors on the drone and achieved better results than GPS positioning. A similar approach was implemented for real-time pose estimation by Hong et al. [16], combining the Cubature Kalman Filter on IMU readings with an optical-flow-based correction to minimize positioning error.

2.3. Computer Vision for AR

For successful AR use and application, a detailed understanding of the scene is required, a challenging task that includes multiple sensor fusion, object tracking and real, and virtual world registration [17]. Computer Vision approaches have been used in AR applications for object detection and tracking [18,19], object pose estimation [20], localization [21], and even gaze-based UAV navigation [22]. In our application, we utilize computer vision techniques for visual pose drone detection [23].

2.4. Situation Awareness and Virtual Information Visualization in AR

Situation awareness (SA) is related to the perception and comprehension of a dynamic environment. Increased SA is related to improved performance and efficiency in the completion of complex tasks and operations. According to Endsley's definition [24], SA comprises three main phases: perception of the relevant elements, their relation to the operation goals, and projection of the operation environment future states. In the context of disaster response and law enforcement operations, drones can provide a means to expand SA by providing video and images from advantageous vantage points [25,26]. Leveraging AR visualization and tools can have positive effects in SA as task-relevant information and feedback can be displayed on the same screen and in the context of real-world elements. The user can easily correlate the augmented information elements with the real world, avoiding additional cognitive load. Earlier work [27,28] has leveraged AR for vehicle operators in maritime applications. In the AR environment, information from maps, radars, and other instruments were fused with the real world view. Their results indicate improved SA of the operators. Lukosch et al. [29] used AR to support information exchange for operational units in the security domain. Their results showed improved SA for personnel that were not present in the scene.

2.5. Visualization in Context

Apart from visualizing virtual information with the aim of improved perception and SA, another key element in our application area is live video in contextualized mixed reality. Cameras are nowadays ubiquitous and used for a wide space of applications, quite often deploying multiple cameras at once. Having multiple views from an observed area, while useful, can also be straining for the observer who, in order to understand the situation, needs to mentally reconstruct the observed area and understand the spatial relations between the different views. In order to reduce this mental workload, new design approaches should be identified. Brejcha et al. [30] introduced a pipeline for aligning photographs in a reconstructed 3D terrain based on location and rotation metadata included in the photographs. The produced result offers improved spatial orientation and scene understanding and overall an enhanced first-person experience for the viewers. Wang et al. [31], suggested and tested different visualization techniques for embedding videos in a 3D spatial environment. One of their preferred approaches is the Billboard video view. In this approach, the video is projected in a rectangle that orients itself in order to face the user. A modified Billboard approach is utilized in our AR application.

3. Architecture

3.1. Overview

As stated in Section 1, the main focus of this work is to provide drone pilots with intuitive gesture control, drone tracking in AR, and a video feed displayed in context with the real environment. This section presents the system architecture developed (depicted in Figure 1) to support these functionalities.

The two end-points of the system are the pilot and the drone. The pilot interacts with the system via an autonomous mixed reality headset that provides hand-tracking capabilities along with visualization in AR. A HoloLens application was developed to support gesture acquisition, give feedback to the pilot, display the received video feed and the drone's tracked position in AR, and handle connectivity and common settings. The drone connects with the system via a direct wireless link with its remote controller, which is connected to a smartphone running a custom Android app to support the needed functionalities. These include transmitting telemetry data from the drone to the AR device and control commands from the AR device to the drone. The communication between the AR device and the drone is routed through a message broker, while the video data are streamed via a direct socket connection between the smartphone and the AR device.

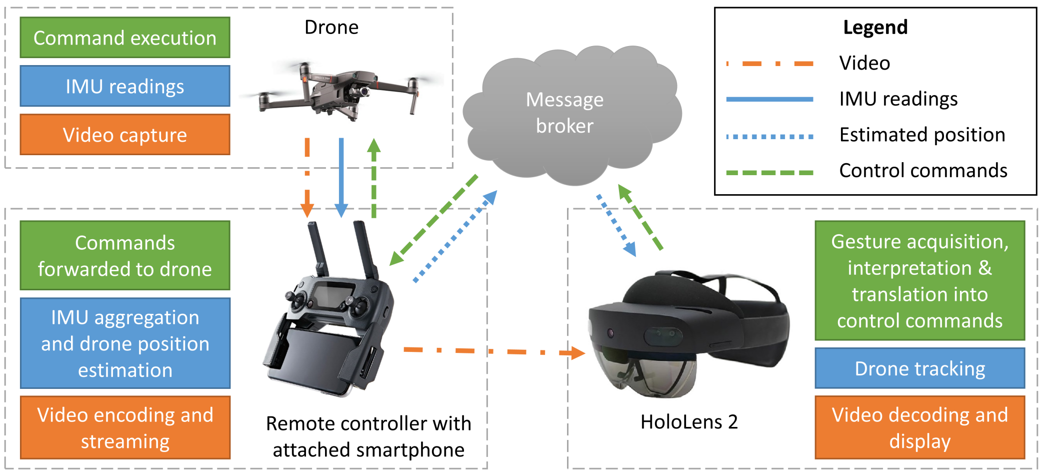
Command execution
IMU readings
Video capture
Drone
Message broker
Legend
Video
IMU readings
Estimated position
Control commands
Commands forwarded to drone
IMU aggregation and drone position estimation
Video encoding and streaming
Remote controller with attached smartphone
HoloLens 2
Gesture acquisition, interpretation & translation into control commands
Drone tracking
Video decoding and display

Figure 1. System architecture and data flow between components.

There are three primary data flows pertinent to the desired functionalities:

- Hand gestures are captured, interpreted, translated to drone commands, and forwarded to the drone.
- Telemetry data are used to estimate the drone's current position, which is then sent to the AR device.
- Live video is captured by the drone's camera, transmitted to the remote controller, and then streamed to the AR device directly.

The remainder of this section further describes the individual system components and their functionalities, while the next section (Section 4) provides technical details regarding the main components of the solution.

3.2. Hardware

The main hardware devices used in the proposed solution are the drone, and the AR device used as a user-interface, both of which are briefly described below. Additional hardware, such as the smartphone connected to the drone's remote and the computer server hosting the message broker, are generic and need no further elaboration.

Developing and testing the architecture was performed using DJI's Mavic 2 Enterprise Dual and Mavic Mini drones. The DJI Mobile SDK platform offers high-level control of the aircraft and the camera–gimbal system, low latency video feed retrieval from the camera, and state information about the aircraft and the controller through various sensors, all of which are essential for development. For outdoor testing, we primarily used the larger Mavic 2 Enterprise Dual drone with its onboard obstacle avoidance system, which was important for safety reasons when implementing gesture control. For indoor testing, the smaller and lighter Mavic Mini was used.

Microsoft's HoloLens 2 was used as an augmented reality platform. HoloLens is a head-mounted system that can display virtual objects in the real world, with the use of two see-through holographic displays. It has a plethora of onboard sensors to understand its surrounding environment (spatial mapping) including four RGB cameras, which combined with a Time-of-Flight Depth sensor, are used to track the user's hands. In addition, two infrared cameras are tracking the user's eyes, optimizing object rendering, and a microphone array can be used to issue voice commands. We capture hand tracking data through the HoloLens interface and translate them into UAV commands to control the drone and the camera. We also use the head tracking information the HoloLens provides to rotate the drone in accordance to head movement. HoloLens was selected because it provides three features necessary for the presented application: AR visualization, hand tracking, and autonomous operation (i.e., not tethered to a computer).

3.3. Communication

Information exchange between the different modules of the presented architecture is achieved via the Kafka (https://kafka.apache.org/, accessed on 20 December 2021) message broker. We use Confluent's implementation (https://www.confluent.io/, accessed on 20 December 2021), which includes a built-in REST proxy and a corresponding API, which are necessary since there are no Kafka clients compatible with UWP (Universal Windows Platform) and the HoloLens. The broker's contents are organized into topics, and each topic corresponds to different functionality of the system (e.g., control commands, positioning info, etc.). The messages abide by the JSON protocol, which is natively supported by Kafka, and their structure is strictly defined. This not only ensures compatibility between modules but also provides significant modularity since new message types can be added, removed, or modified in future versions since they comply with the same JSON structure. Finally, our modules use HTTP operations (POST, GET) to produce and consume the stated messages.

3.4. Augmented Reality Application

The augmented reality app was developed for HoloLens using Unity3D (https://unity.com/, accessed on 20 December 2021) and the Mixed Reality Toolkit (https://github.com/microsoft/MixedRealityToolkit-Unity, accessed on 20 December 2021). The main functional modules of the application are as follows:

- **Drone control commands**: This module is responsible for capturing the gesture/voice interactions of the user, translating them to specific control commands (i.e., pitch, roll, yaw, and throttle values), and sending them to the the Android app via the Kafka broker.
- **Drone tracking**: The drone tracking module is responsible for monitoring the spatial relation between the real world elements (the drone and the app user) and its virtual representatives. Drone tracking is the backbone for many feedback cues (visual, textual, contextualized videos) that provide the user with enhanced spatial perception. Tracking is possible following an initial calibration process and an IMU-based approach.
- **Video feedback**: The live video feed from the drone's camera is projected on a canvas inside the augmented environment. The user can simultaneously be aware of his/her surroundings in the real environment while also viewing the drone's video feed in his/her field of view (FoV). With minimal head movement and loss of focus, the user can perceive the surrounding environment from two different viewpoints. This video projection is modifiable and can either be placed in the center of the user's FoV as shown in Figure 2 (FPV mode) or on a smaller panel projected from the drone's virtual counterpart (Figure 3). The center placement is useful in tasks where higher detail of the drone's camera feed is required. This contextualized video feed mode is called "egocentric" view with the drone at the center and allows for easier perception of what the drone "sees" during the flight and of the spatial correspondence between the drone's and the user's point of view. In contrast, the FPV mode is useful in tasks where higher detail of the drone's camera feed is required. In addition, when using a drone equipped with an infrared camera, the user can choose between three different modalities, visible (RGB), infrared (IR), or fused (MSX).
- AR feedback and visualization: GUI elements and various visualization features were added in the AR application to provide feedback and various controls. Emphasis was given to creating an easy-to-use application and increasing the SA of the user. In more detail:
  – Visualization of the virtual hand joints overlaying on top of the user hands, making it possible for the user to directly check if his/her hands are correctly perceived by HoloLens (Figure 4).
  – Drone visualization based on the drone tracking module. A virtual drone is overlaid on top of the real drone so that the user is aware of the drone's relative

position even if it is not in a direct line of sight (e.g., behind a wall or building) or too far to be easily visible with a naked eye.

- An extensive virtual menu that includes all high level commands and toggles for enabling the application features is present in the lower part of the application view. The menu can be be hidden in order to not obstruct the user's field of view.
- A navigation feedback panel is placed at the top part of the application's window. In the feedback panel, the current perceived navigation commands are listed alongside with other drone- and user-related information such as the drones's flying altitude and horizontal distance from the user, the drone heading, and the user heading.

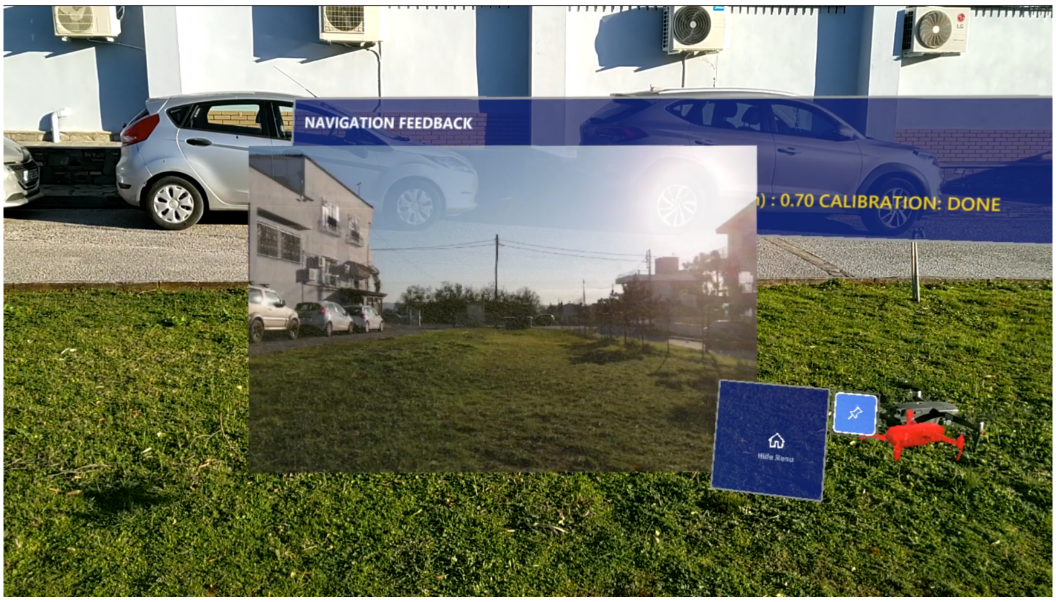

): 0.70 CALIBRATION: DONE

Figure 2. First Person View (FPV) into the Augmented Reality environment. Real and virtual drones are shown in the lower right corner.

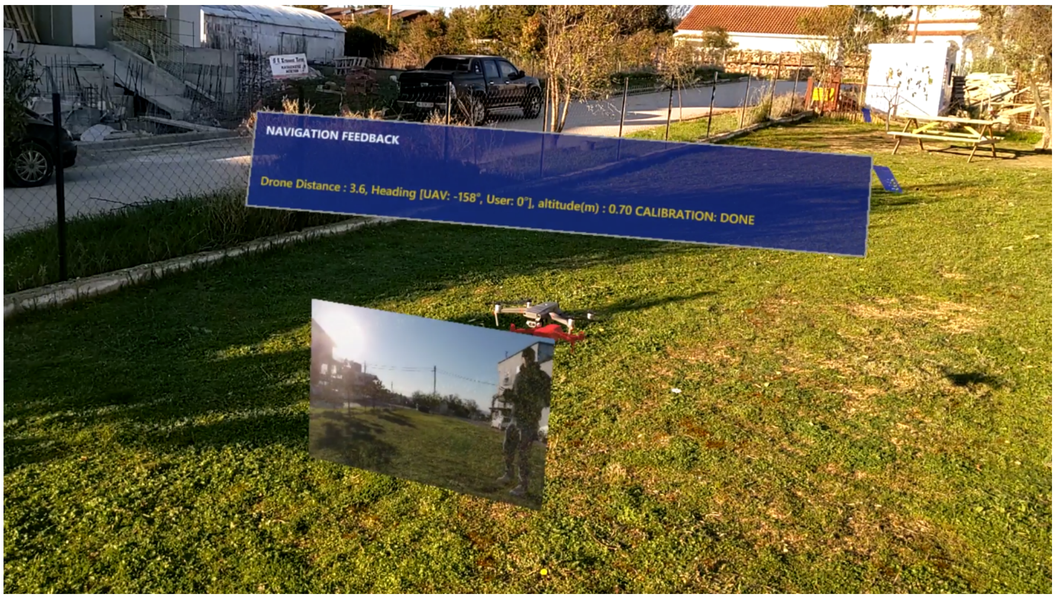

Drone Distance : 3.6, Heading [UAV: -158°, User: 0°], altitude(m) : 0.70 CALIBRATION: DONE

Figure 3. The AR Egocentric View mode. The AR user can be shown in collinearity between the user and the drone's camera in the right corner.

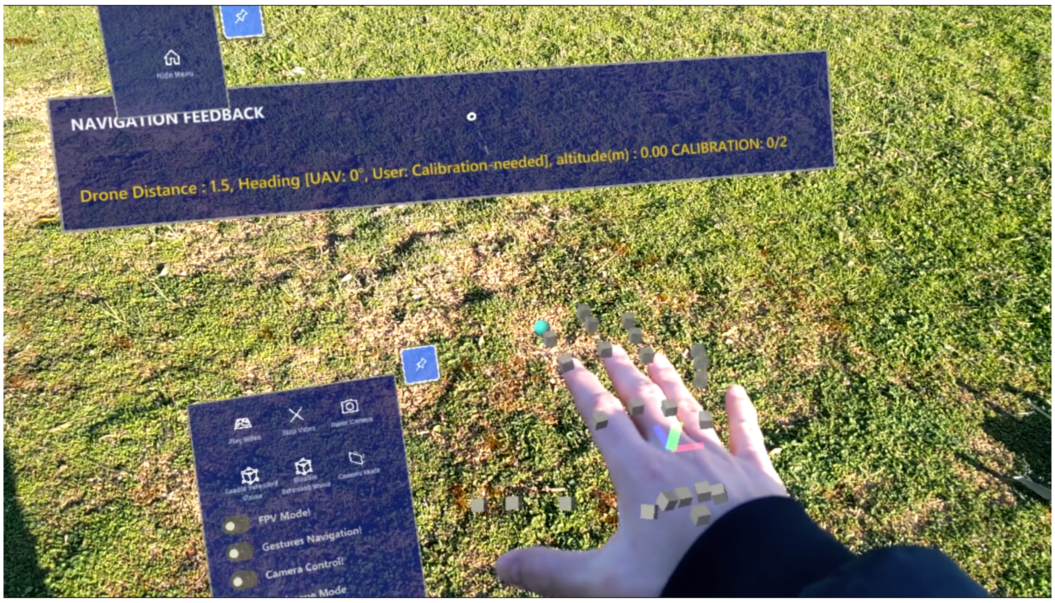
NAVIGATION FEEDBACK

Drone Distance : 1.5, Heading [UAV: 0°, User: Calibration-needed], altitude(m) : 0.00 CALIBRATION: 0/2

Figure 4. Hand-tracking as visualized in our AR application. Cubes represent hand joints. (The displacement of joints is due to the location of camera capturing the screenshots; the user of the app can see the virtual joints on top of his/her actual joints.

3.5. UAV Interface Application

An application was developed to act as a communication bridge between the DJI drone and the rest of the system architecture. We chose the Android platform since it was the most mature and versatile Mobile SDK platform DJI had to offer at the time of development. The app is installed on an Android smartphone connected to the remote controller via a USB cable. The drone connects to the remote controller via DJI's proprietary communication protocol, OcuSync, while the smartphone connects to the rest of the system by WiFi or a commercial mobile network. The app's primary responsibilities are:

1. Receiving control commands from Kafka and forwarding them to the drone;
2. Collecting the drone's IMU readings, aggregating them to estimate its position, and posting this to Kafka at regular intervals;
3. Sending the drone's live video feed directly to the HoloLens via network sockets.

The application, depicted in Figure 5, displays practical information (e.g., battery status of the aircraft and of the remote controller), along with a live view of the drone's camera feed. Buttons are also present to perform various actions. The "Configurator" button exposes the user to a settings page shown on the left pane of Figure 5, where several parameters can be configured, including connection settings, the sensitivity of the drone to gesture commands, and infrared visualization options.

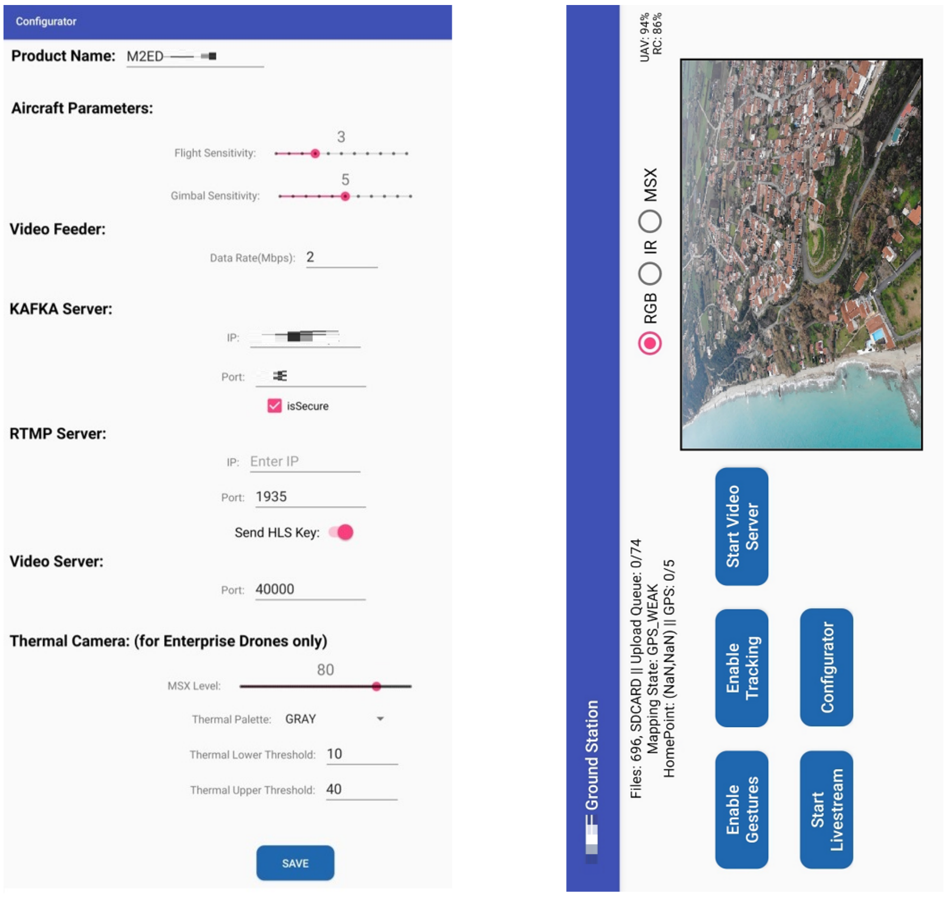
Configurator

Product Name: M2ED[redacted]

Aircraft Parameters:

Flight Sensitivity: 3

Gimbal Sensitivity: 5

Video Feeder:

Data Rate(Mbps): 2

KAFKA Server:

IP: [redacted]

Port: [redacted]

☑ isSecure

RTMP Server:

IP: Enter IP

Port: 1935

Send HLS Key: ●

Video Server:

Port: 40000

Thermal Camera: (for Enterprise Drones only)

MSX Level: 80

Thermal Palette: GRAY

Thermal Lower Threshold: 10

Thermal Upper Threshold: 40

UAV: 94%
RC: 86%

[✓ RGB] IR MSX

Files: 696, SDCARD || Upload Queue: 0/74
Mapping State: GPS_WEAK
HomePoint: (NaN,NaN) || GPS: 0/5

Figure 5. The Android UAV interface app. Left: the app's configurator page, with setting regarding connectivity, gesture command sensitivity, and infrared view display. Right (rotated): the app's main view, showing a live view of the drone's camera feed.

4. Methodology

The realization of the presented solution can be broken down into five tasks, each regarding a different aspect of the gesture control or the AR visualization pipeline:

- **Gesture definition**, in which an appropriate set of hand gestures was selected to control the drones, meeting requirements relating both to usability and control. This was the focus of earlier work ([32]), refined and updated for the current work;
- **Gesture acquisition**, in which users' hand gestures must be captured, interpreted, translated to flight or camera control commands, and forwarded to the drone via the UAV interface Android app;
- **Drone position tracking in AR**, in which the drone's motions must be tracked in reference to the virtual world, based on aggregated IMU reading and optionally improved by visual cues;
- **Calibration**, in which the virtual environment must be aligned with the real world, in terms of both translation and rotation, so that virtual objects can be displayed in the context of the environment. Calibration is necessary both for tracking and displaying the drone in AR and displaying a contextualized video feed, which depends on tracking;
- **Video transmission and visualization**, in which the drone's video feed must be transmitted to the HoloLens and displayed in AR in (near) real time, via the UAV interface Android app.

The rest of this section describes in detail each of these five tasks, presenting the methodologies followed, noting weaknesses, and outlining possible future improvements.

4.1. Gesture Definition

4.1.1. Requirements and Considerations

In order to develop a viable alternative drone control system, it should allow users to perform the same motions as a regular handheld remote: pitch, roll, yaw, throttle, and their combinations, as well as camera motions. Similarly, it should allow users to define the sensitivity of each command, and by extension, the amplitude of the corresponding motion.

Designing Natural User Interfaces (NUI), such as gestures, some additional requirements must be taken into account to achieve intuitive interaction. Peshkova et al. [33] explained that the gestures should be related to each other while following a single metaphor. In the same study, the use of multi-modal interaction, such as a combination of gesture and speech commands, is encouraged in order to increase naturalness. Hermann et al. [11] additional requirements were highlighted including avoidance of non-ergonomic positions (as described in [34]) and the presence of some form of feedback. In an AR environment, several forms of feedback can be integrated in the real-world view of the user as overlaid virtual objects.

Hence, UAV gesture control has three primary aims:

1. To provide an easy-to-learn and intuitive interface;
2. To be physically comfortable and ergonomic;
3. To allow the full extent of drone motions, including combination motions and variable velocities.

4.1.2. Gesture Vocabulary

In a previous user study and survey [32], we tested two sets of gesture vocabularies, a finger-based and a palm-based vocabulary in a simulated drone navigation environment. Users were required to navigate a virtual drone in an outdoor and an indoor environment. In the finger-based mode, each gesture is defined by which fingers are extended, and the velocity value is defined by the pointing direction of a selected extended finger. In the palm-based mode, the operator uses the positioning and orientation of his/her open palm (all finders extended) to control the drone. The subjective study results showed a clear user preference for the palm-based control, which was described as more comfortable and easier to learn and use. The objective metrics showed faster task completion using the palm-based controls, however, finger-based control offered more precise navigation. The overall objective score showed that the palm-based control has a slightly better performance.

The study results are aligned with findings in [33] that intuitive NUIs should be based on a common metaphor. In this case, the metaphor chosen is that the drone corresponds to the user's hand, and hence mimics and follows all its movements. Therefore, raising the hand up higher will correspond to an ascend (increase throttle) command; a tilt of the hand will correspond to the drone assuming a similar angle (pitch and/or roll); a horizontal rotation will correspond to yaw; and so on. This metaphor, validated by the user study, addresses the first aim of gesture control.

The second aim of gesture control is to avoid non-ergonomic, physically stressing hand gestures. It may be noted that even easy-to-perform gestures can be tiring when performed repeatedly or may oblige users to hold their hand/arm steady in the same height for a long time. In order to avoid the latter, we applied a relative gesture vocabulary based on a varying reference position. One key gesture is used as a reset and calibration command. When the user performs this key hand gesture, the current hand pose is set as the neutral (resting) position, and all following gestures are interpreted relative to this. This allows users to chose the resting position that is most comfortable to them and even define new resting positions in preparation for certain maneuvers.

Hence, a user wishing to command the drone to ascend may define a low resting position, allowing her to move her hand higher with no discomfort. Later, in preparation for a descent, a higher resting position may be chosen so that the user can lower her hand easily. The reset and calibration command is tied to the user opening the palm and extending the fingers. Hence, after a brake and stop command (closed fist), a new resting position is always defined before the user issues a new command. While the hand is closed and no commands are issued, users can position their hand in preparation for the next gestures safely.

This palm-based gesture set was expanded in later work to include take-off and landing gestures [35]. Similar to a handheld remote, these gestures are mapped to hand positions assumed and held over a couple of seconds. To differentiate them from the other UAV control commands, take-off and landing use an upwards-facing palm. The full palm gesture vocabulary used for drone navigation is shown in Figure 6. Moreover, the user's other hand can be used to control the camera gimbal, where the same set of gestures are mapped to camera pitch and yaw.

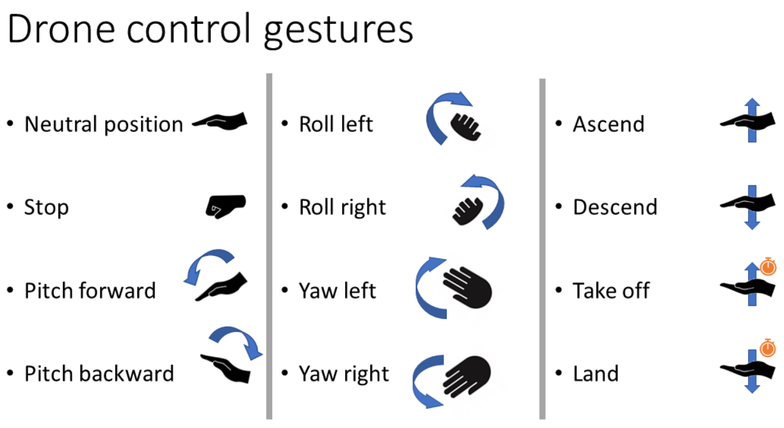

Figure 6. The palm gesture vocabulary used for drone navigation.

It can be noted that the selected gesture set can be used to perform any UAV motion achievable with the traditional handheld remote. Velocities of UAV commands are mapped directly to the angles or distances relative the resting position, allowing for a continuous control ranging from no motion at all to fast motion. Combination motions, such as pitching forward while yawing a little to the left and slowly descending are easily achievable. This can be further substantiated, as the human hand, like all real-world objects, has six degrees of freedom (translation and rotation along three axes), while a quadcopter's control has four (pitch, roll, yaw, and throttle). This demonstrates that movements are independent of each other and can hence be freely combined. Naturally, the same holds for the camera-controlling hand. Therefore, the third aim of gesture control is addressed.

4.1.3. Drone Control Features

The drone control module was implemented following an agile development process; starting from a set of basic features, continuous testing and user feedback led to the refinement of the user requirements. Initially, the ***hand gesture drone control*** was implemented and three additional features, ***hand gesture camera control***, ***periscope*** mode, and high-level ***voice control*** commands were added.

The primary task was to accurately navigate the drone using the selected palm gestures. It should also be noted that when no gesture is performed or when the user hand is not visible, no command is sent, and the drone stops. Inside the AR application, visual cues were displayed providing feedback to facilitate the navigation task. Drone navigation is performed using the user's right hand by default, however, this can be a parameter.

In the hand gesture camera control, the unassigned user hand, by default the left hand, is used for controlling the view direction of the drone's camera. This feature is controlling the camera gimbal, which is able to perform 2DoF movements: rotation up/down (pitch) and rotation right/left (yaw). The gesture vocabulary used for camera control is similar to the vocabulary for drone navigation, however, there are less defined gestures since the camera's possible movements are fewer; by tilting the open palm left or right, the camera turns to the corresponding direction in the vertical axis while, by tilting the palm up or down, the camera rotates in the corresponding direction in the horizontal axis.

Periscope mode is an additional form of gesture control, which does not involve the use of hands but it is based on the user's head direction. When Periscope mode is enabled, the drone viewing direction follows the user's head direction in real time. For example, when the user rotates his head to look 90° east, the drone rotates to the exact same direction. Periscope is an auxiliary feature allowing for a quick and intuitive inspection of the surrounding environment that has collected very positive reviews from the end-users.

Finally, voice commands are used to perform high-level commands such as resetting the camera direction. Voice commands are completely optional, as all the commands can be alternatively performed by buttons and controls available in the virtual application menu, however, they offer a multi-modal tool of interaction and at the same time allow the user to use their hands for controlling the drone or perform an other task and at the same time dictate the desired command using speech.

4.2. Gesture Acquisition

4.2.1. Background

Our early research [32] into gesture acquisition for drone control considered two different hardware peripherals: the AvatarVR glove (https://avatarvr.es/, accessed on 20 December 2021), a wearable with embedded IMU and touch sensors, and the LeapMotion controller (https://developer.leapmotion.com/, accessed on 20 December 2021), an infrared LED and camera device. The former was found to falsely report finger curl when rotating the hand, which made it incompatible with the open hand metaphor described in the previous subsection; hence, it was discarded for the current application. The LeapMotion controller performed well in a lab setting but the lack of wireless portability (as it needs a USB connection) and its inability to track hands in an sunlit outdoor environment were important limiting factors. However, it served well for the initial development phase of the solution, as it includes a Unity API. Most of the gesture recognition and interpretation functions were based on the LeapMotion API and later adapted for the HoloLens.

Google's MediaPipe Hands [36] was also considered for purely RGB-camera-based gesture acquisition. This has proved robust in a wide range of lighting conditions, making it suitable both indoors and outdoors. However, as it is compatible with Unix and Android systems only, the integration of this modality into the HoloLens has not been realized. It has been used with a webcam for training on a computer simulator, and it could be considered for future developments on different AR devices or standalone gesture control applications not including AR visualization.

4.2.2. Gesture Acquisition and Interpretation in HoloLens 2

Gesture recognition for the palm-based control in HoloLens 2 utilized the MRTK Unity3D plugin and more specifically, the Hand-tracking API. The MRTK hand-tracking API did not provide (at least during the time of the development) high-level functions for recognizing extended fingers or an open/closed palm. The main values provided are handedness (left or right hand), joint transform (the position and orientation in the 3D space), and joint type (e.g., index tip, index distal, metacarpals, etc.). As a result, the development of palm navigation had to start by implementing a Gesture Recognizer component able to detect an open palm gesture in real-life conditions where fingers are quite often occluded or not completely straight, etc. The gesture recognizer component is based on the work provided by Rob Jellinghaus (https://github.com/RobJellinghaus/MRTK_HL2_HandPose/, accessed on 20 December 2021), but is heavily modified to adjust to our case needs. The code takes into account finger–eye alignment and co-linearity between finger pairs to cope with finger occlusions. It also uses ratios between different hand's parts instead of absolute measurements to be able to handle different hand sizes. Since in the palm-based control we are only interested in two classes of gestures, open/extended palm and closed palm, the gesture detector does not have to be very precise in recognizing gesture details. For that reason, the gesture classification criteria are modified to match the needs of the application: The criterion for an open palm classification is the detection of an extended thumb and at least three extended fingers. This way, the recognizer is more sensible in recognizing an open palm gesture, which is the main state of interest.

When the Gesture Recognizer module detects an open palm, the hand joints' information (position and rotation) is processed by the Palm Navigation module that calculates the navigation commands (pitch, yaw, roll, throttle, and take off/landing) and their amplitude (or velocity values) based on the hand joints' current and past rotation angles. As mentioned in Section 4.1.2, in order to avoid physical stress, the reference null position can change every time the user performs the reset command (closed palm gesture). The next open palm position after the reset command corresponds to the reference position and the joint angles and position at that point are stored as the neutral (or zero) transforms for the future commands.

In particular, three components of the hand's position are relevant: the hand's Up normal vector, perpendicular to the palm; the hand's Forward normal vector, perpendicular to Up, and facing forward, along the direction of the middle finger; and the hand's vertical position. An overview of the vectors and their correspondence with the drone control values is shown in Figure 7. Interpretation is relative to the reference hand position. The current position's normals are translated to the y-axis and analyzed into components. Pitch is computed by the angle of the Forward vector to the xz-plane. Yaw is tied to the angle of the Forward vector's xz-component to the x-axis. Roll is computed by the angle of the Up vector's yz-component to the y-axis. Throttle is proportionate to the vertical (y-axis) distance between the current position and the reference. All commands allow for a "neutral zone", so that minor or involuntary motions are not translated to a drone command.

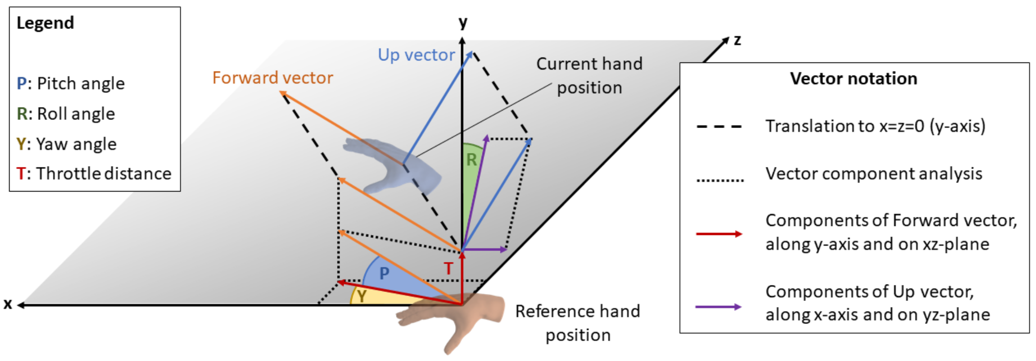
Legend
P: Pitch angle
R: Roll angle
Y: Yaw angle
T: Throttle distance
y
z
x
Up vector
Forward vector
Current hand position
Reference hand position
P
R
Y
T
Vector notation
Translation to x=z=0 (y-axis)
Vector component analysis
Components of Forward vector, along y-axis and on xz-plane
Components of Up vector, along x-axis and on yz-plane

Figure 7. Palm vectors and angles used to interpret gesture commands. Interpretation is always relative to the reference position, whose normal vectors form the axes x, y, and z. The current position's normals are translated to the y-axis and analyzed into components. Pitch, roll, yaw, and throttle values are then computed according to the angles and distances between these component vectors and the reference axes.

4.3. Drone Position Tracking in AR

Drone tracking is used to monitor the physical location of the drone during a flight. In our case, this information is utilized in two different ways: to assist monitoring and piloting the drone when it is out of line of sight or too distant to distinguish it clearly using a virtual drone marker in the AR environment and to position the AR video canvas according to the drone's location and orientation and hence in context with the real environment.

Drones are commonly equipped with two positioning mechanisms: GPS and IMU. GPS is commonly used to provide an approximate location-based satellite communication. However, it presents two major drawbacks: It is only available outdoors, and its precision is limited, ranging from 2.5 m to 10 m or more [14]. This precision can be inadequate for flights that require precision. Hence, the presented system relies on IMU readings. The DJI SDK offers no access to low-level IMU measurements; instead, it combines the readings from multiple sensors, including magnetometer, gyrospope, and accelerometer measurements to report the estimated velocity of the drone, at regular intervals. Velocity is reported in a North–East–Down (NED) coordinate system, with an origin point at the drone's starting location. The reported velocity measurements V are collected by the Android UAV interface app, multiplied by the interval time T to yield translations in distance, and summed to provide the estimate position of the drone D at time t, relative to its starting point:

$$D_t = \sum_{i=0}^{t} D_i = \sum_{i=0}^{t} V_i T_i \tag{1}$$

The above assumes that between reports, velocities remain constant, which is not the case when performing maneuvers. However, with a 100 ms reporting period, these errors are negligible. A more significant drawback to this procedure is the low precision — two decimal places—at which velocities are reported by the SDK. This makes for an average error of 0.005 m/s. Naturally, this becomes more significant at lower velocities, where it can account for up to 16% of the real velocity. Even without compensation, the position as derived by aggregated IMU readings is more accurate than GPS over short periods of time and short distances. With the error-correcting compensation described in Section 5, the accuracy improves significantly and is adequate for both locating and guiding the drone, perhaps excluding very precise maneuvering in tight spaces. For longer distances, GPS reading can be used correctively to ensure that the aggregated IMU drift is capped to the GPS precision.

The application posts the position related data presented in JSON format on the Kafka broker. The post frequency is four times per second in order to consume less network and computational process power. On the client side, the HoloLens application connects to the Kafka broker and consumes these messages on a specific topic. Based on the message information, it renders a virtual drone-like object into the augmented reality environment, overlaying the position of the real drone. In order to achieve this coupling, a prior calibration process is required to align the HoloLens's internal coordinate system with that of the drone.

4.4. Calibration of the AR Environment

Tracking a real object in augmented reality and visualizing it in context with the real environment requires a correspondence between two different coordinate systems: one based in the real world and one based in the virtual world, which will be superimposed on the real world to provide the AR graphics. As outlined in Section 4.3, the drone's position is continuously estimated based on aggregated IMU readings and its heading is supplied directly by its onboard compass. Hence, the calculated pose is expressed in relation to a system of coordinates with the drone's starting location as an origin point and its y-axis aligned with the north.

The HoloLens does not use its internal compass to orient its internal coordinate system, and the compass readings are not readily available to Unity apps. Therefore, the AR elements, including the virtual drone marker and the video panel, must be expressed in relation to the internal coordinate system, with an origin and y-axis direction equal to that at the user's location and heading, respectively, at the time of launching the application.

In order to link the two coordinate systems and place the virtual drone marker in the corresponding position of the physical drone and, by extension, for the video panel to be displayed correctly in context with the environment, a calibration procedure should be performed. The calibration process aims to calculate the relative translation and rotation between the two systems. Even though both real and virtual objects are mobile in 3D, with six DoF, the drone's altitude is tracked and reported independently via its altimeter. Hence, this can be viewed as a 2D problem of axis rotation and translation.

Keeping elementary linear algebra in mind [37], for two 2D coordinate systems with the same alignment (no rotation) and an offset of x'_0, y'_0, if x, y are the coordinates of a point in one system, then its coordinates in the rotated system will be:

$$\begin{bmatrix} x' \\ y' \end{bmatrix} = \begin{bmatrix} x \\ y \end{bmatrix} + \begin{bmatrix} x'_0 \\ y'_0 \end{bmatrix} \tag{2}$$

Meanwhile, for two 2D coordinate systems with the same origin point (no translation) and a rotation of ϕ, if x, y are the coordinates of a point in one system, then its coordinates in the rotated system will be:

$$\begin{bmatrix} x' \\ y' \end{bmatrix} = \begin{bmatrix} cos(\phi) & sin(\phi) \\ -sin(\phi) & cos(\phi) \end{bmatrix} \begin{bmatrix} x \\ y \end{bmatrix} \tag{3}$$

In the generic case of both translation and rotation, we have:

$$\begin{bmatrix} x' \\ y' \end{bmatrix} = \begin{bmatrix} cos(\phi) & sin(\phi) \\ -sin(\phi) & cos(\phi) \end{bmatrix} \begin{bmatrix} x \\ y \end{bmatrix} + \begin{bmatrix} x'_0 \\ y'_0 \end{bmatrix} \tag{4}$$

Hence, using the real-world drone and its virtual marker in the AR coordinate system as the common point, we can link the two coordinate systems following a calibration procedure. The following text describes both the default, manual calibration method and two vision-based alternatives.

4.4.1. Manual Two-Step Calibration

The manual two-step calibration method relies on users performing the HoloLens's "air tap" gesture to mark the drone's location to the HoloLens app.

In the generic case, the HoloLens app will launch with the user some distance away from the drone and facing a random direction, forming an angle ϕ with the north. Figure 8 shows the two different coordinate systems and the devices' starting location with different colors. In order to translate coordinates from one system to the other, we need to calculate the coordinates of the origin of one with respect to the other (translation vector) and the angle ϕ, which can form the rotation matrix.

During the first step of calibration, the drone has not yet moved, and the user air-taps its present (starting) position, as shown in Figure 8 on the left. That position's HoloLens coordinates (x_0^H, y_0^H) are then captured and stored and form the translation vector.

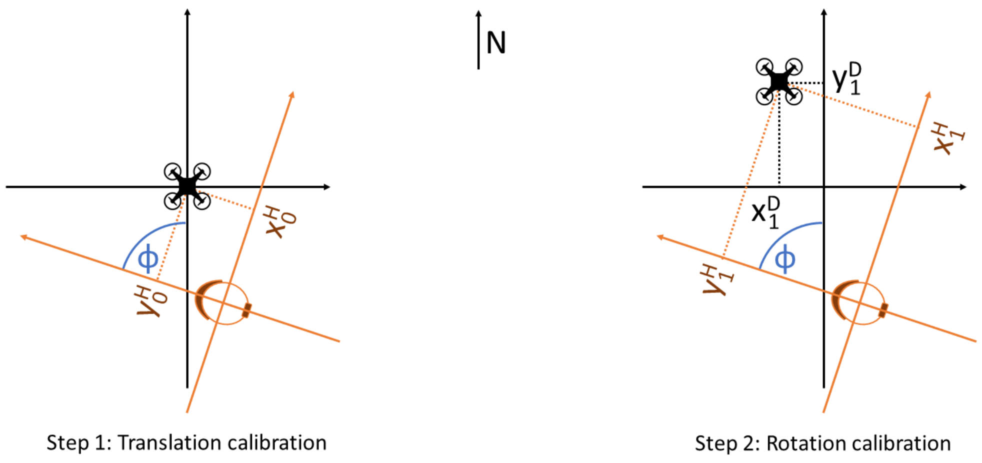

Figure 8. Axis translation and rotation via the two-step manual calibration process. Left: with the first tap on the drone, the translation offset is captured by the HoloLens. Right: after moving the drone a small distance, the second tap captures the drone's position in both coordinate systems (HoloLens and Drone), allowing the calculation of rotation angle ϕ.

To capture the rotation angle, the drone is moved from its starting position. The new position's HoloLens coordinates (x_1^D, y_1^D) are captured with a second air-tap. At the same time, the new position's Drone coordinates (x_1^H, y_1^H) are calculated based on the aggregated IMU readings. Figure 8, on the right, shows this second step. Hence, Equation (4) yields:

$$\begin{bmatrix} x_1^H \\ y_1^H \end{bmatrix} = \begin{bmatrix} cos(\phi) & sin(\phi) \\ -sin(\phi) & cos(\phi) \end{bmatrix} \begin{bmatrix} x_1^D \\ y_1^D \end{bmatrix} + \begin{bmatrix} x_0^H \\ y_0^H \end{bmatrix} \tag{5}$$

The only unknown being ϕ, the above can yield:

$$\begin{aligned} cos(\phi) &= \frac{x_1^H - sin(\phi) y_1^D - x_0^H}{x_1^D} \\ sin(\phi) &= \frac{x_1^H y_1^D - x_1^D y_1^H - x_0^H y_1^D + x_1^D y_0^H}{(x_1^D)^2 + (y_1^D)^2} \end{aligned} \tag{6}$$

Therefore, Equation (6) can be used to obtain rotation angle ϕ, given any non-zero displacement (x_1^D, y_1^D). Knowing both translation and rotation, any future drone-system coordinates can be translated to HoloLens system coordinates to allow visualization in AR.

4.4.2. Visual Drone Pose Estimation

Instead of relying on user information (air-taps) a drone's relative pose (position and orientation) may be inferred from visual data, captured live from the HoloLens's onboard camera. To that end, we propose a method that exploits the latest advances in deep learning to automatically retrieve the 6DoF pose of a drone from a single image. An early version of this architecture, described in more detail in [23], uses a CNN encoder backbone followed by three fully connected layers that output two predictions, one for the translation components and one for the rotation. The translation prediction uses an L_2 loss, while the rotation prediction aims to minimize the angular difference L_R. The two loss functions are weighted by a balancing hyperparameter λ and combined to form the training loss function.

The newest update employs a state-of-the-art architecture, HRNet [38], as a landmark regression network to predict the eight landmark image positions. Then, we retrieve the pose using the predicted 2D–3D correspondences. However, this approach does not permit end-to-end training, as the pose retrieval step is not differentiable. Towards this end, we exploited the recently introduced BPnP algorithm [39], which has been proved to be effective for the pose estimation task [40].

For training our models and evaluating their performance, we have compiled and made publicly available the UAVA dataset (also in [23]), an extensive set of synthetic, photorealistic images of drones in indoor and outdoor environments, which provides ground truth annotations of 2D keypoints, pose, depth maps, normal maps, and more.

Accurate visual drone pose estimation can automate and simplify the calibration process, as both distance (step 1) and orientation (step 2) can be estimated by a single image, automatically, without user input. Visual recognition of the drone and its pose by HoloLens is robust at distances of a maximum of 5–10 m, depending on drone model and size. In addition, this method can be used to periodically correct the position computed by the aggregated IMU readings, offsetting IMU drift and any other errors. With the current version specifications of HoloLens, such an algorithm cannot run continuously in real time. However, even sparse inferences, performed every 5–15 s, can keep IMU drift at a minimum and improve tracking.

4.4.3. QR Code Reading

An alternative to the visual estimation of the drone's pose is to rely on QR codes pasted on the physical drones. The HoloLens provides a built-in capability to detect and read QR codes robustly. Hence, by pasting a QR code on top of the drone, the HoloLens can detect its starting position (analogous to step 1 in the manual calibration process) automatically, with no need of human intervention. While the air-tap determines a single point and hence provides only position information, the QR code is an object, and its detection can provide both position and orientation. Hence, in conjunction with the heading provided by the drone's compass, both steps of the manual calibration process can be completed in a single QR code read.

Naturally, a QR code pasted on a drone's top is easily readable at short distances (perhaps a maximum of 2 m), i.e., while the drone is landed and the user stands close to it. Hence, while this method can provide fast and automated calibration, it cannot be used for correcting the drone's position during flight and offsetting IMU drift, as is the case with Section 4.4.2.

4.5. Video Transmission and Visualization

When implementing the live streaming feature of the drone's camera video feed to HoloLens 2, we had to consider specific requirements regarding latency and frame rate. In order for the video stream to be usable for piloting, it had to be low in latency and high in frame rate. Overall latency is the sum of two values: the latency from the drone to the remote controller, which depends on the drone manufacturer and the streaming protocols used, and the latency from the remote controller to the HoloLens, via the UAV interface app, which depends on the presented solution. In this case, DJI uses OcuSync for video transmission, which adds a nominal latency of 120 to 270 ms. The following text focuses on the latency between the remote controller and the HoloLens.

Ideally, the overall latency should be low enough to allow easy and safe control based solely on the video feed (e.g., in FPV mode) and frame rate should be high enough for the video to be viewable as a continuous stream. Therefore, we set targets for <350 ms overall latency (hence 120 ms for the Android-to-HoloLens latency) and >15 frames per second (FPS).

4.5.1. Video Streaming

Several methods and streaming protocols were considered for the transmission of live video to the HoloLens, including Real-Time Messaging Protocol (RTMP), Real-time streaming protocol (RTSP), sending frames as individual messages through Kafka, and direct connection via network sockets.

RTMP is a flash-based video streaming protocol routing the video stream through a server and supported natively by the DJI SDK. However, RTMP induces high latency, ranging from one to several seconds, depending on the the network conditions and server location and capabilities. This makes RTMP a good choice for non-reactive video watching (e.g., for a spectator) but unsuitable for remote control. RTSP and HLS (Http Live Streaming) exhibit similar behavior, and hence they were discarded for use in the presented solution.

Sending video frames through Kafka was implemented in an effort to simplify the architecture by routing all data through the same hub (Kafka). Two flavors were tested: sending encoded frames directly from the UAV interface app to the HoloLens and decoding the frames first on Android and then forwarding the decoded data to the HoloLens. Naturally, the first flavor minimizes bandwidth requirements, while the second minimizes the processing strain on the HoloLens. On a local (Wi-Fi) network, bandwidth is less of a concern, hence latency was reduced when streaming decoded frames. However, the frame rate has proved to be too low (at about 11 FPS) in both cases. This is attributed to the HoloLens using a REST API to connect to Kafka (as there are no clients available for UWP), which induces an overhead for each message request. Therefore, this approach was also discarded.

The solution finally selected made use of Network Sockets. This type of connection is Point-to-Point, meaning that once the connection is established, no additional overhead is required for the flow of data. With this implementation, in contrast to the two previous methods, there is no intermediate server between the drone and the HoloLens. The Android device running the UAV interface app acts as a server with the HoloLens being the client. To test this approach, we connected the drone and the HoloLens to alleviate network bottlenecks. We measured the Android-to-HoloLens latency below 100 ms and the frame rate exactly 30 FPS, which is the native frame rate of the drone's camera. Since both requirements were met, this method is the most appropriate for piloting the drone through the live video feed from the camera.

4.5.2. Video Decoding

On the HoloLens side, the decoding process starts when the connection has been established. For the purposes of the decoding task, we have implemented a dedicated library using the FFmpeg tool, namely, Decoder, to handle video frames. The library has been implemented as a dynamic-link library for the Microsoft Windows operating system and built for UWP architecture compatible with HoloLens 2.

The Android app feeds the AR app with h.264 encoded frames. In the AR application decoding and visualization of the received video frames are handled in two background processing threads. The first thread runs the Decoder module while the second thread is responsible for the frame visualization. Decoding is performed in a 30Hz (native) rate while rendering in 15Hz for performance reasons and efficient management of computational resources. Rendered frames are displayed in a virtual projection panel. In contextualized video mode, this panel is placed in front of the drone, in the direction its camera is facing, while in FPV mode it is centered on the user's field of view.

During development, different methods of video streaming were implemented and tried (as shown in Figure 9). These included RTMP streaming (top left), sending video frames through Kafka (top right), and a direct connection using web sockets (bottom). The latter was finally selected, as it yields the lowest latency and requires no intermediaries.

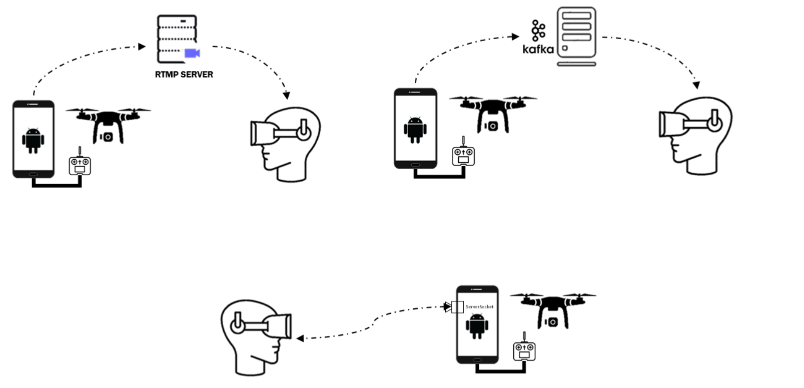

Figure 9. Diagrams of different streaming methods.

5. Testing and Evaluation

The presented solution was tested both subjectively and objectively. Subjective tests included a pre-development user study to define the gesture set used for drone control and a number of field trials where users had a chance to try the system in action. Objective measurements concerned the responsiveness time between gesture execution and drone reaction, IMU-based tracking error, and the latency in video transmission. Each of the above is presented in the following subsections.

5.1. Subjective User Evaluation

5.1.1. Gesture Usability

The gestures and underlying metaphor were selected in a pre-development user study, including a survey resulting from both subjective and objective measurements. Two gesture sets were considered: the palm-based gesture, where the drone mimics the orientation of the user's palm, and a finger-based gesture set with no common underlying metaphor, where three different commands (pitch, yaw, and throttle) were mapped to distinct gestures, differentiated by which fingers are extended. The study aimed to define a finger-based gesture set and then measure user preference and performance in the two gesture sets: the mutually exclusive, rigidly defined finger-based gestures, and the freer and combinable palm-based gestures.

The study, conducted between December 2019 and February 2020, included two parts. The first part aimed to define the finger-based gesture set. Based on a questionnaire completed by 29 participants, we selected those finger-based gestures voted as both comfortable and intuitively appropriate and mapped them to the 3 drone control commands.

The second part employed a drone flight simulator developed in Unity and coupled with a gesture acquisition peripheral and gesture interpretation programming. It aimed at measuring the ease of learning, usability, and comfort of each control mode, as well as the performance in terms of mission completion time and collision avoidance. An outdoor and an indoor scene were prepared for testing. Participants, including 27 men and 12 women with varying degrees of familiarity with drone control, were asked to control a virtual drone in the simulator and pass through specific waypoints while avoiding collision with walls. Each participant tried both modes (palm- and finger-based) and both types of scenes (indoor and outdoor). Both objective and subjective results were obtained: the former by measuring the timings and collision from the simulator itself and the latter via a questionnaire.

An overview of the results can be seen in Figure 10. The results showed an overall preference for palm-based control. This included both faster timings and less collisions, and a subjective evaluation of it being easier to learn and more comfortable to use. In contrast, finger-based control was generally slower, but could be more precise, and hence useful in very tight environments (e.g., indoors). For more information and further results, the interested reader is referred to the full user study publication [32].

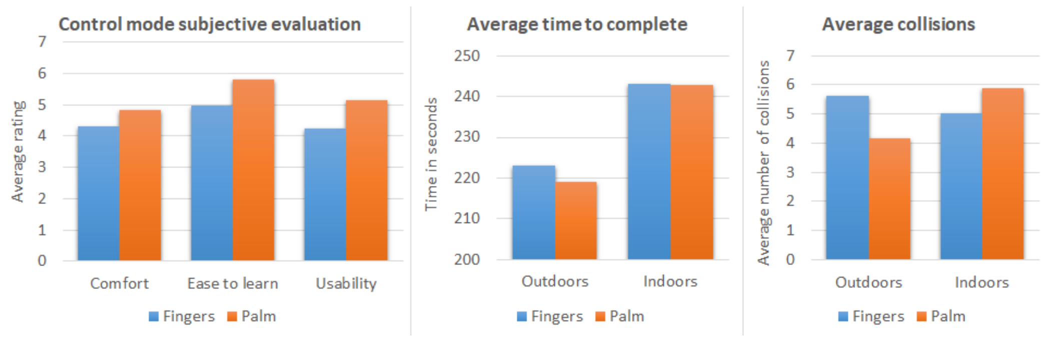

Figure 10. Overview of the gesture selection user study results.

5.1.2. Field Trials

Post-development, the complete system has been demonstrated to both drone pilots and non-expert users. While these evaluations are still ongoing, early results are being used to guide adjustments and improvements in the system. In these events, participants are first responders interested in using drones for search-and-rescue operations. Such mission are often stressful, highlighting the need for more comfortable and intuitive drone control and a video feed easily viewed and placed in context. Early demonstration and feedback sessions have been held in Japan (July 2021—9 participants), Greece (October 2021—6 participants), and France (November 2021—12 participants), with additional events planned for Italy, Finland, and Spain in the first half of 2022.

Initial feedback from these events indicate that gesture control with a real drone is easy to learn for inexpert users, comfortable, and allows full control, including any maneuver possible with a handheld remote. One setback noted concerned the use of the HoloLens in very bright sunlight or a hot day: Both of these conditions degraded the HoloLens's hand-tracking performance, and the heat caused it to shut down after a few minutes. This is expected, as the HoloLens employs passive cooling and is designed primarily for indoor use. However, under non-extreme heat and sunlight conditions, performance has been consistent and robust.

Two experienced drone pilots taking part in the demonstrations stated that they would feel comfortable using gesture control, provided conditions did not degrade the robustness of the HoloLens's hand tracking. The periscope mode, which keeps the drone motionless while tying its yaw to that of the HoloLens, has proven particularly popular and useful for scanning an area.

Regarding drone tracking in AR, feedback was mixed: The manual calibration process, in particular, often proves too difficult and complicated for users. This feedback has driven a turn towards implementing a easier, largely automated, vision-based calibration process, relying on AI visual pose estimation and/or QR codes, as described in Section 4.4. The new calibration process will be tested and evaluated in upcoming demonstration events.

Concerning visualization, users preferred the FPV mode rather than the contextualized view mode. This has been in part due to the difficult calibration process, which is a prerequisite for drone tracking and hence contextualized display. In addition, the size of the contextualized display was sometimes deemed too small. Based on this feedback, future versions will feature a larger canvas on which to display the video feed, as well as the option to scale this canvas using gestures on the camera-controlling hand.

5.2. Lab Testing and Objective Measurements

5.2.1. Drone Responsiveness

When testing alternative drone control methods, an important consideration is the response time of the drone. In the presented solution, this is the latency between the user performing a gesture and the drone responding to this command. In the presented architecture, commands are transmitted from the HoloLens to the UAV interface app via a Kafka broker on the Internet or a local network. The location of the broker, as well as network conditions, can impact drone response latency.

To measure this latency, a high-speed camera was used to capture both the user and the drone at 240 frames per second, also described in previous work [35]. Over a series of experiments, a counting of the number of elapsed frames between the user's gesture and the drone reaction yielded average latency timings. Different locations of the Kafka broker were considered and measured separately: the broker being on the same local network as the HoloLens and the UAV interface; the broker being in a different city in the same country; and the broker being in a different country. Figure 11 shows the minimum and the average timings measured in these experiments. With a camera frame rate of 240 frames per second, measurement error is less than 5 ms, which has has no significant impact on the conclusions of this experiment.

Since a DJI drone consumes commands from its remote controller every 40–200 ms, that degree of latency is unavoidable. In a local area network, the observed latency was minimal, at less than 200 ms, therefore, no worse than that of conventional, handheld remote controls. At more remote broker locales, response latency increases. However, even at around 300 ms, it is still within acceptable limits for drone piloting.

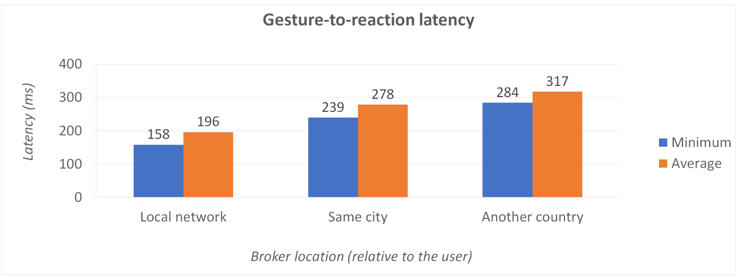

Figure 11. Drone response time measurements according to broker location.

5.2.2. Positioning Accuracy

The basic modality of drone tracking calculates the drone's position based on the IMU readings it reports. Even small error from individual reading aggregate over time resulting in IMU drift. Hence, any error correction or compensation can improve the robustness of the system in a span of seconds or minutes.

To measure IMU positioning accuracy, an experiment was conducted where the drone would move forward close to ground level and the position as calculated from the IMU readings would be compared to the actual distance traveled, measured physically on the ground. The experiment was repeated for different values of pitch, corresponding to different velocities.

The results of these experiments are presented in Figure 12. The position estimated from the IMU is marked on the horizontal axis, while the ground truth is on the vertical. For reference, the yellow diagonal line marks the ideal of zero error, where IMU measurements equal the ground truth. It can be noted that the error is relatively small for higher pitch values and velocities, increasing when the drone moves slower. This is also evident by the angles of the different linear trendlines. For pitch = 0.3, the trendline is almost parallel to the zero-error line, while for lower pitches, the lines diverge. It may also be noted that IMU measurements steadily report a smaller than the actual distance. Using linear regression, the functions of each trendline can be calculated. In the following, GT is the ground truth, and IMU is the distance measured by the IMU readings aggregation:

$$\begin{aligned} GT &= 1.31 * IMU + 0.20,\ for\ pitch = 0.05 \\ GT &= 1.17 * IMU + 0.27,\ for\ pitch = 0.1 \\ GT &= 0.99 * IMU + 0.217,\ for\ pitch = 0.3 \end{aligned} \tag{7}$$

The observations of Figure 12 may be used to improve the IMU measurements by compensating for the error. As noted, this compensation must be inversely tied to the pitch value. Performing linear regression on the coefficients of Equation (7), we can approximate them as a function of the respective pitch value as $1 + (1/52.36 * pitch)$. As the $GT = IMU$ equation (with a coefficient of 1) is the ideal (i.e., no error), the $1/52.36 * pitch$ part expresses the error of the measurements.

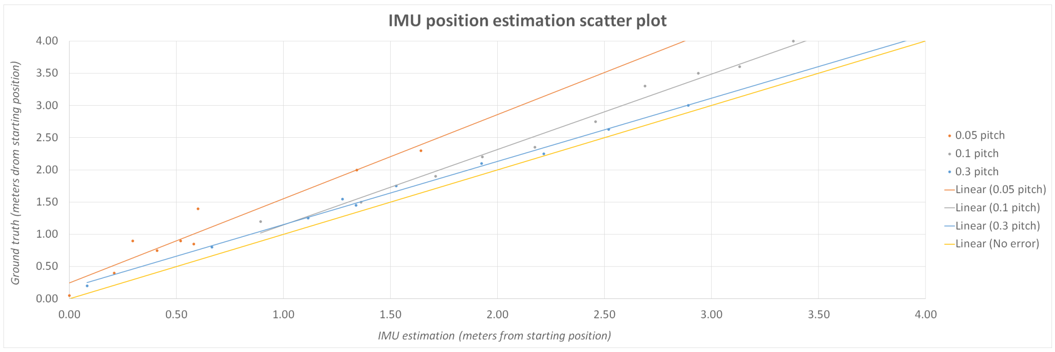

Figure 12. IMU measurements vs. ground truth for various pitch values, including linear trendlines and a no-error line for reference. Note how lower pitch values result in greater errors, and how the angle between the trendlines and the no-error line increases for slower speeds.

Hence, a simple, first-degree estimation of the error E per distance unit would be:

$$E = \frac{1}{52.36 * pitch} \tag{8}$$

Therefore, the compensated distance D_{comp} can be calculated from the measured distance D as:

$$D_{comp} = D * (1 + E) = D * (1 + \frac{1}{52.36 * pitch}) \tag{9}$$

Figure 13 shows the effect of error compensation on IMU measurements. The left graph shows the mean squared error (MSE) of measurements for different pitch values, without compensations (solid lines) and with (dashed lines). The right graph shows the average MSE values for the different pitch values, again, with and without compensation. It can be seen that compensation has a huge impact, especially on lower pitches (slower drone speeds).

Compensation research is still ongoing. Future tests will include combination motions and different drone models, as well as higher-degree error modeling.

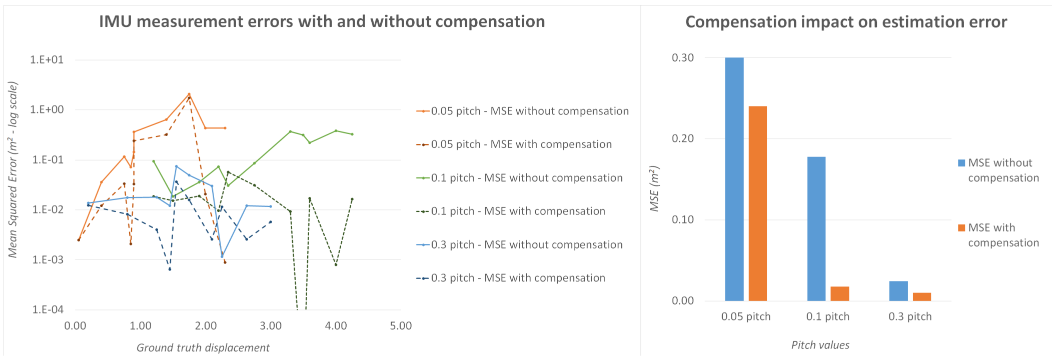

Figure 13. IMU measurement compensation. (**Left**): MSE of the error without compensation (solid lines) and with (dashed lines) for different pitch values. Note that the vertical axis is in logarithmic scale. (**Right**): Comparison of average MSE values with and without compensation, for different pitch values. Compensation has a drastic impact on slower speeds, where the error is greatest.

5.2.3. Video Transmission

A final measurement regarded the latency and frame rate of video transmission and display. End-to-end latency was measured, as above, with a high-frame-rate camera, which yielded an average measurement of 467 ms. While such latency is acceptable for inspection or searching, it is not ideal for piloting a drone in FPV, based on video feedback only. Video transmission latency can be considered in two steps: from the drone to the UAV interface app connected to the remote controller and from there to the HoloLens. The first part was measured at 386 ms, accounting for the larger part of the overall latency. However, this is significantly greater than the timings reported by DJI (170–240 ms) (https://www.dji.com/gr/mavic-mini/specs, accessed on 20 December 2021). Further investigation into this could result in decreased video latency. A full frame rate of 30 frames per second (native to the drone's camera) was achieved.

6. Conclusions and Future Steps

6.1. Conclusions

In this paper, we have presented a unified system for AR-integrated drone use, encompassing gesture control, tracking, and camera feed visualization in context with the user's environment. We have outlined the overall system architecture as well as individual components, described the mechanics of the vital tasks necessary for its function and conducted both objective and subjective evaluation experiments. Different aspects of the proposed solution were evaluated, with the results described in Section 5, including gesture selection and usability; drone responsiveness in terms of time lag; drone tracking accuracy and the efficacy of compensation; and video transmission quality.

Although the presented implementation focused on specific hardware (the HoloLens and DJI drones), the underlying logic and architecture are modular and not tied to the current hardware choices. As mentioned in the Section 4.2, the same gesture control methodology has been implemented and tested successfully with alternative hardware, including a regular webcam or smartphone camera. Hence, integration with different drone models or AR hardware is possible and mostly a matter of implementation.

The presented system has largely achieved its objectives, and future plans include both refinements and wider validation. In particular, gesture control has proved both intuitive and accurate, providing the same level of control as a traditional handheld remote.

However objective evaluation with real drones (i.e., not a simulator) has not yet been completed and is scheduled for the near future. This should be in comparison with the handheld remote controller, with pilots being asked to place the drone in a specified position. Measurements could include accuracy (distance from the specified position) and time (to achieve that position). In addition, more complex drone behaviors can be tied to either specific gestures or virtual buttons in future implementations; such behaviors can include flying in a circular or other pattern or returning to land either at the take-off location or near the user.

6.2. AR Tracking and Visualization Present and Future Vision

Work into the AR components—drone tracking, calibration, and visualization—of the presented solution is still ongoing. While the currently developed system is a working prototype, a number of possible future improvements have been outlined and planned for the medium term.

Figure 14 presents our vision for such future additions.

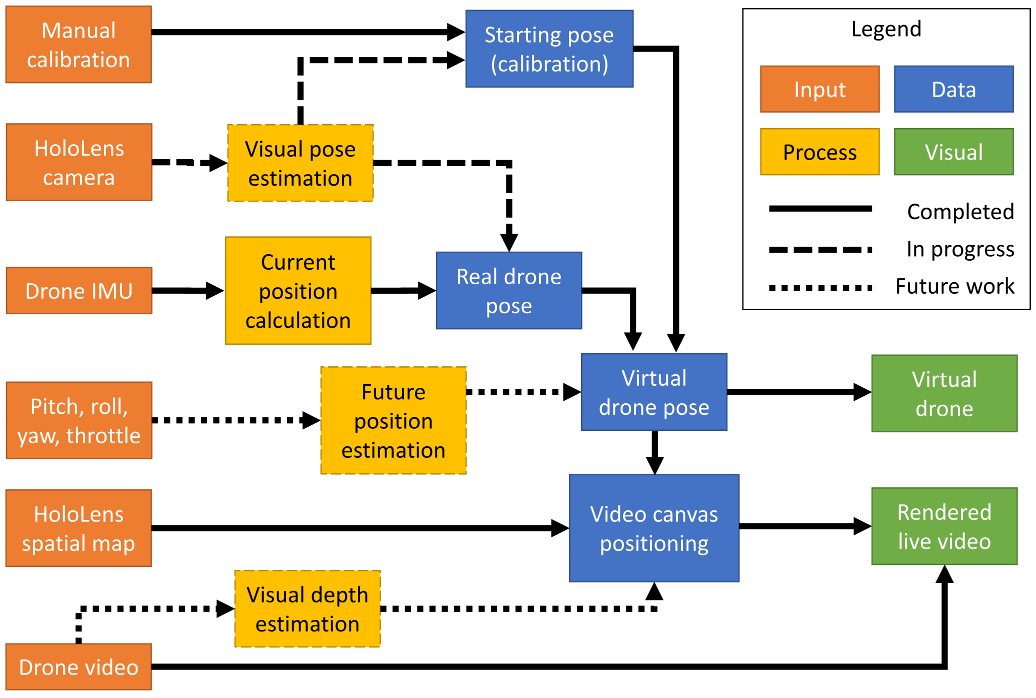

Figure 14. Present and future components of the AR part of the solution. Solid lines indicate completed modules, dashed lines work in progress, and dotted lines future plans.

Regarding calibration, the working prototype uses a manual, two-step calibration, which can prove both tiresome and challenging for inexpert users. Hence, work is already in progress to calibrate initial drone pose with a largely automated, visual method. Two options are currently considered, as outlined in the Section 4.4: a visual drone pose estimation AI and the reading of QR codes pasted on the drones. The former should also provide intermittent visual recognition of the drone during flight, correcting the IMU readings and eliminating any accumulated drift.

In addition, it can be noted that the position as tracked in AR will always lag some time behind that of the real drone, as IMU readings must be collected, read, and aggregated, a position estimated and forwarded to the HoloLens and there displayed. A future module could raw input from the flight control of the drone (pitch, roll, yaw, and throttle) and estimate a future position for the drone, offsetting the lag of data transmission and processing.

Finally, the AR video canvas is currently displayed a set distance in front of the virtual (tracked) drone. However, the actual distance between the drone and the objects in its field of view might range from a couple of meters to hundreds. A depth estimation algorithm could gauge this distance and position the video canvas appropriately, for a more realistic display in context with the environment.

Author Contributions: Conceptualization, K.K., G.A. and A.D.; data curation, D.T. and G.A.; formal analysis, K.K. and D.T.; funding acquisition, A.D. and P.D.; investigation, K.K. and D.T.; methodology, K.K. and K.C.; project administration, A.D. and P.D.; resources, A.D. and P.D.; software, K.C., D.T. and D.S.; supervision, K.K., A.D. and P.D.; validation, K.K.; visualization, D.S.; writing—original draft, K.K., K.C., D.T., D.S. and G.A.; writing—review and editing, K.K., K.C., A.D. and P.D. All authors have read and agreed to the published version of the manuscript.

Funding: This research has been supported by the European Commission within the context of the project FASTER, funded under EU H2020 Grant Agreement 833507.

Informed Consent Statement: Informed consent was obtained from all subjects involved in the study.

Acknowledgments: The authors would like to thank the Hellenic Rescue Team Attica (HRTA—Greece) and the École Nationale Supérieure des Officiers de Sapeurs-Pompiers (ENSOSP—France) for testing the proposed system in the context of search-and-rescue operations and providing valuable feedback. Additional thanks are due to drone operators Michail Fotoglou and Eleni Antoniou for testing the gesture control system during its development and offering feedback from an experienced operator's point of view.

Conflicts of Interest: The authors declare no conflict of interest.

References

1. Özaslan, T.; Loianno, G.; Keller, J.; Taylor, C.J.; Kumar, V.; Wozencraft, J.M.; Hood, T. Autonomous navigation and mapping for inspection of penstocks and tunnels with MAVs. *IEEE Robot. Autom. Lett.* **2017**, *2*, 1740–1747. [CrossRef]
2. Shihavuddin, A.; Chen, X.; Fedorov, V.; Nymark Christensen, A.; Andre Brogaard Riis, N.; Branner, K.; Bjorholm Dahl, A.; Reinhold Paulsen, R. Wind turbine surface damage detection by deep learning aided drone inspection analysis. *Energies* **2019**, *12*, 676. [CrossRef]
3. Wu, K.; Rodriguez, G.A.; Zajc, M.; Jacquemin, E.; Clément, M.; De Coster, A.; Lambot, S. A new drone-borne GPR for soil moisture mapping. *Remote Sens. Environ.* **2019**, *235*, 111456. [CrossRef]
4. Hill, A.C. Economical drone mapping for archaeology: Comparisons of efficiency and accuracy. *J. Archaeol. Sci. Rep.* **2019**, *24*, 80–91. [CrossRef]
5. Joyce, K.; Duce, S.; Leahy, S.; Leon, J.; Maier, S. Principles and practice of acquiring drone-based image data in marine environments. *Mar. Freshw. Res.* **2019**, *70*, 952–963. [CrossRef]
6. Karjalainen, K.D.; Romell, A.E.S.; Ratsamee, P.; Yantac, A.E.; Fjeld, M.; Obaid, M. Social drone companion for the home environment: A user-centric exploration. In Proceedings of the 5th International Conference on Human Agent Interaction, Bielefeld, Germany, 17–20 October 2017; pp. 89–96.
7. Mishra, B.; Garg, D.; Narang, P.; Mishra, V. Drone-surveillance for search and rescue in natural disaster. *Comput. Commun.* **2020**, *156*, 1–10. [CrossRef]
8. Burke, C.; McWhirter, P.R.; Veitch-Michaelis, J.; McAree, O.; Pointon, H.A.; Wich, S.; Longmore, S. Requirements and Limitations of Thermal Drones for Effective Search and Rescue in Marine and Coastal Areas. *Drones* **2019**, *3*, 78. [CrossRef]
9. Tezza, D.; Andujar, M. The State-of-the-Art of Human–Drone Interaction: A Survey. *IEEE Access* **2019**, *7*, 167438–167454. [CrossRef]
10. Suárez Fernández, R.A.; Sanchez-Lopez, J.L.; Sampedro, C.; Bavle, H.; Molina, M.; Campoy, P. Natural user interfaces for human-drone multi-modal interaction. In Proceedings of the 2016 International Conference on Unmanned Aircraft Systems (ICUAS), Arlington, VA, USA, 7–10 June 2016; pp. 1013–1022. [CrossRef]
11. Herrmann, R.; Schmidt, L. Design and Evaluation of a Natural User Interface for Piloting an Unmanned Aerial Vehicle: Can gestural, speech interaction and an augmented reality application replace the conventional remote control for an unmanned aerial vehicle? *i-com* **2018**, *17*, 15–24. [CrossRef]
12. Kleinschmidt, S.P.; Wieghardt, C.S.; Wagner, B. Tracking Solutions for Mobile Robots: Evaluating Positional Tracking using Dual-axis Rotating Laser Sweeps. In Proceedings of the ICINCO 2017, Madrid, Spain, 26–28 July 2017; pp. 155–164.
13. Islam, S.; Ionescu, B.; Gadea, C.; Ionescu, D. Indoor positional tracking using dual-axis rotating laser sweeps. In Proceedings of the 2016 IEEE International Instrumentation and Measurement Technology Conference Proceedings, Taipei, Taiwan, 23–26 May; IEEE: Piscataway, NJ, USA, 2016; pp. 1–6.

14. Arreola, L.; De Oca, A.M.; Flores, A.; Sanchez, J.; Flores, G. Improvement in the UAV position estimation with low-cost GPS, INS and vision-based system: Application to a quadrotor UAV. In Proceedings of the 2018 International Conference on Unmanned Aircraft Systems (ICUAS), Dallas, TX, USA, 12–15 June; IEEE: Piscataway, NJ, USA, 2018; pp. 1248–1254.
15. Tsai, S.E.; Zhuang, S.H. Optical flow sensor integrated navigation system for quadrotor in GPS-denied environment. In Proceedings of the 2016 International Conference on Robotics and Automation Engineering (ICRAE), Jeju, Korea, 27–29 August; IEEE: Piscataway, NJ, USA, 2016; pp. 87–91.
16. Hong, Y.; Lin, X.; Zhuang, Y.; Zhao, Y. Real-time pose estimation and motion control for a quadrotor uav. In Proceedings of the 11th World Congress on Intelligent Control and Automation, Shenyang, China, 29 June–4 July 2014; IEEE: Piscataway, NJ, USA, 2014; pp. 2370–2375.
17. Hoff, W.A.; Nguyen, K.; Lyon, T. Computer-vision-based registration techniques for augmented reality. In *Intelligent Robots and Computer Vision XV: Algorithms, Techniques, Active Vision, and Materials Handling*; International Society for Optics and Photonics: Bellingham, WA, USA, 1996; Volume 2904, pp. 538–548.
18. Deshmukh, S.S.; Joshi, C.M.; Patel, R.S.; Gurav, Y. 3D object tracking and manipulation in augmented reality. *Int. Res. J. Eng. Technol.* **2018**, *5*, 287–289.
19. Shreyas, E.; Sheth, M.H.; Mohana. 3D Object Detection and Tracking Methods using Deep Learning for Computer Vision Applications. In Proceedings of the 2021 International Conference on Recent Trends on Electronics, Information, Communication Technology (RTEICT), Bangalore, India, 27–28 August 2021; pp. 735–738. [CrossRef]
20. Rambach, J.; Deng, C.; Pagani, A.; Stricker, D. Learning 6DoF Object Poses from Synthetic Single Channel Images. In Proceedings of the 2018 IEEE International Symposium on Mixed and Augmented Reality Adjunct (ISMAR-Adjunct), Munich, Germany, 16–20 October 2018; pp. 164–169. [CrossRef]
21. Li, J.; Wang, C.; Kang, X.; Zhao, Q. Camera localization for augmented reality and indoor positioning: A vision-based 3D feature database approach. *Int. J. Digit. Earth* **2020**, *13*, 727–741. [CrossRef]
22. Yuan, L.; Reardon, C.; Warnell, G.; Loianno, G. Human Gaze-Driven Spatial Tasking of an Autonomous MAV. *IEEE Robot. Autom. Lett.* **2019**, *4*, 1343–1350. [CrossRef]
23. Albanis, G.; Zioulis, N.; Dimou, A.; Zarpalas, D.; Daras, P. Dronepose: Photorealistic uav-assistant dataset synthesis for 3D pose estimation via a smooth silhouette loss. In *European Conference on Computer Vision*; Springer: Cham, Switzerland, 2020; pp. 663–681.
24. Endsley, M.R. Toward a Theory of Situation Awareness in Dynamic Systems. *Hum. Factors* **1995**, *37*, 32–64. [CrossRef]
25. Silvagni, M.; Tonoli, A.; Zenerino, E.; Chiaberge, M. Multipurpose UAV for search and rescue operations in mountain avalanche events. *Geomat. Nat. Hazards Risk* **2017**, *8*, 18–33. [CrossRef]
26. Volckaert, B. Aiding First Incident Responders Using a Decision Support System Based on Live Drone Feeds. In Proceedings of the Knowledge and Systems Sciences: 19th International Symposium, KSS 2018, Tokyo, Japan, 25–27 November 2018; Springer: Berlin/Heidelberg, Germany, 2018; Volume 949, p. 87.
27. Hong, T.C.; Andrew, H.S.Y.; Kenny, C.W.L. Assessing the Situation Awareness of Operators Using Maritime Augmented Reality System (MARS). *Proc. Hum. Factors Ergon. Soc. Annu. Meet.* **2015**, *59*, 1722–1726. [CrossRef]
28. Rowen, A.; Grabowski, M.; Rancy, J.P. Through the Looking Glass(es): Impacts of Wearable Augmented Reality Displays on Operators in a Safety-Critical System. *IEEE Trans. Hum.-Mach. Syst.* **2019**, *49*, 652–660. [CrossRef]
29. Lukosch, S.; Lukosch, H.; Datcu, D.; Cidota, M. Providing information on the spot: Using augmented reality for situational awareness in the security domain. *Comput. Support. Coop. Work (CSCW)* **2015**, *24*, 613–664. [CrossRef]
30. Brejcha, J.; Lukác, M.; Chen, Z.; DiVerdi, S.; Cadík, M. Immersive trip reports. In Proceedings of the 31st Annual ACM Symposium on User Interface Software and Technology, Berlin, Germany, 14–17 October 2018; pp. 389–401.
31. Wang, Y.; Krum, D.M.; Coelho, E.M.; Bowman, D.A. Contextualized Videos: Combining Videos with Environment Models to Support Situational Understanding. *IEEE Trans. Vis. Comput. Graph.* **2007**, *13*, 1568–1575. [CrossRef] [PubMed]
32. Konstantoudakis, K.; Albanis, G.; Christakis, E.; Zioulis, N.; Dimou, A.; Zarpalas, D.; Daras, P. Single-Handed Gesture UAV Control for First Responders—A Usability and Performance User Study. In Proceedings of the 17th International Conference on Information Systems for Crisis Response and Management (ISCRAM 2020), Blacksburg, VA, USA, 24–27 May 2020; Volume 17, pp. 937–951.
33. Peshkova, E.; Hitz, M.; Kaufmann, B. Natural Interaction Techniques for an Unmanned Aerial Vehicle System. *IEEE Pervasive Comput.* **2017**, *16*, 34–42. [CrossRef]
34. Nielsen, M.; Störring, M.; Moeslund, T.B.; Granum, E. A Procedure for Developing Intuitive and Ergonomic Gesture Interfaces for HCI. In *Gesture-Based Communication in Human-Computer Interaction*; Camurri, A., Volpe, G., Eds.; Springer: Berlin/Heidelberg, Germany, 2004; pp. 409–420.
35. Sainidis, D.; Tsiakmakis, D.; Konstantoudakis, K.; Albanis, G.; Dimou, A.; Daras, P. Single-handed gesture UAV control and video feed AR visualization for first responders. In Proceedings of the 18th International Conference on Information Systems for Crisis Response and Management (ISCRAM 2021), Blacksburg, VA, USA, 23–26 May 2021; Volume 18, pp. 835–848.
36. Zhang, F.; Bazarevsky, V.; Vakunov, A.; Tkachenka, A.; Sung, G.; Chang, C.L.; Grundmann, M. Mediapipe hands: On-device real-time hand tracking. *arXiv* **2020**, arXiv:2006.10214.
37. Anton, H.; Rorres, C. *Elementary Linear Algebra: Applications Version*; John Wiley & Sons: Hoboken, NJ, USA, 2013.

38. Sun, K.; Xiao, B.; Liu, D.; Wang, J. Deep high-resolution representation learning for human pose estimation. In Proceedings of the IEEE/CVF Conference on Computer Vision and Pattern Recognition, Long Beach, CA, USA, 15–20 June 2019; pp. 5693–5703.
39. Chen, B.; Parra, A.; Cao, J.; Li, N.; Chin, T.J. End-to-end learnable geometric vision by backpropagating PnP optimization. In Proceedings of the IEEE/CVF Conference on Computer Vision and Pattern Recognition, Seattle, WA, USA, 14–19 June 2020; pp. 8100–8109.
40. Albanis, G.N.; Zioulis, N.; Chatzitofis, A.; Dimou, A.; Zarpalas, D.; Daras, P. On End-to-End 6DOF Object Pose Estimation and Robustness to Object Scale. ML Reproducibility Challenge 2020. 2021. Available online: https://openreview.net/forum?id=PCpGvUrwfQB (accessed on 20 December 2021)